

Respiratory Effort Belts in Postoperative Respiratory Monitoring: Pilot Study with Different Patients

Tiina M Seppänen^{1,2}, Olli-Pekka Alho^{2,3,4}, Merja Vakkala^{2,5}, Seppo Alahuhta^{2,5}
and Tapio Seppänen^{1,2}

¹Center for Machine Vision and Signal Analysis, University of Oulu, P.O Box 4500, 90014 Oulu, Finland

²Medical Research Center Oulu, Oulu University Hospital and University of Oulu, Oulu, Finland

³Department of Otorhinolaryngology, Oulu University Hospital, Oulu, Finland

⁴Research Unit of Otorhinolaryngology and Ophthalmology, University of Oulu, Oulu, Finland

⁵Department of Anesthesiology, Oulu University Hospital, Oulu, Finland

Keywords: Airflow Waveform, Respiratory Airflow, Respiratory Rate, Respiratory Volume.

Abstract: Respiratory complications are common in patients after the general anaesthesia. Respiratory depression often occurs in association with postoperative opioid analgesia. Currently, there is a need for a continuous non-invasive respiratory monitoring of spontaneously breathing postoperative patients. We used calibrated respiratory effort belts for the respiratory monitoring pre- and postoperatively. Used calibration method enables accurate estimates of the respiratory airflow waveforms. Five different patients were measured with the spirometer and respiratory effort belts at the same time. Preoperative measurements were done in the operating room just before the operation, whereas postoperative measurements were done in the recovery room after the operation. We compared three calibration models pre- and postoperatively. Postoperative calibration produced more accurate respiratory airflows. Results show that not only the tidal volume, minute volume and respiratory rate can be computed precisely from the estimated respiratory airflow, but also the respiratory airflow waveforms are very accurate. The method produced accurate estimates even from the following challenging respiratory signals: low airflows, COPD, hypopneic events and thoracoabdominal asynchrony. The presented method is able to produce estimates of postoperative respiratory airflow waveforms to enable accurate, continuous, non-invasive respiratory monitoring postoperatively.

1 INTRODUCTION

Respiratory complications are common in patients after the general anaesthesia. Respiratory depression often occurs in association with postoperative opioid analgesia (Etches, 1994; Gamil and Fanning, 1991; Taylor et al., 2005). Adequate respiration monitoring postoperatively is important, so that respiratory depression can be identified as early as possible (George et al., 2010; Lynn and Curry, 2011).

During general anaesthesia, mechanical ventilation is used and, consequently, monitoring of gas exchange and respiration can be done accurately. During postoperative care, respiratory status can be assessed with oxygen saturation (SpO₂) measurements, blood gas measurements, subjective clinical assessment and intermittent, manual measurements of respiratory rate (Lynn and Curry, 2011; Ramsay et al., 2013). The problems with these

methods are that they are slow and, in addition, subjective methods are also unreliable and give inconsistent results (Lovett, 2005). There is a need for a continuous non-invasive respiratory monitoring of spontaneously breathing postoperative patients. Respiratory depression and subsequent adverse outcomes can arise from pain, residual operating room anaesthetics and administration of opioids for pain management (Cepeda et al., 2003). Inadequate respiration can result in respiratory complications, morbidity, mortality and excessive costs.

A few studies have been recently published on monitoring postoperative respiration continuously and non-invasively. Drummond et al., (2013) have studied respiratory rate and breathing patterns of postoperative subjects using encapsulated tri-axial accelerometer taped to a subject's body. They found that abnormal breathing patterns are extremely common. Voscopoulos et al., (2015; 2014a; 2014b)

have studied minute ventilation, tidal volume and respiratory rate of postoperative subjects using impedance-based electrodes placed to a subject's body.

Recently, we published a novel calibration method to produce accurate estimates of respiratory airflow signals from respiratory effort belt signals (Seppänen, 2013). Here, the method is used in order to produce estimates of postoperative respiratory airflow waveforms to enable accurate, continuous, non-invasive respiratory monitoring postoperatively. Pre- and postoperative measurement data of different patients are used to demonstrate the performance of the method.

2 MATERIALS AND METHODS

2.1 Materials

The study protocol was approved by the Regional Ethics Committee of the Northern Ostrobothnia Hospital District. Five patients who had lumbar back surgery and were expected to need opioid analgesia postoperatively were recruited to the study. Exclusion criteria were BMI (Body Mass Index) over 40 and the planned surgical wound being in the area where respiratory effort belts were placed. The characteristics of the volunteers are given in Table 1.

Table 1: Characteristics of volunteers.

Patient	Gender	Age [years]	BMI [kg/m ²]	Disease
1	M	68	21.8	None
2	M	41	30.3	None
3	F	77	22.4	None
4	M	64	28.1	COPD
5	M	67	27.4	Sleep apnea

Respiratory effort belt signals were recorded with the polygraphic recorder (Embletta Gold, Denver, Colorado, USA). The recorder had inductive respiratory effort belts for rib cage and abdomen with the sampling rate of 50 Hz. For calibrating the respiratory effort belt signals, simultaneous respiratory airflow signal was recorded with a spirometer (Medikro Pro M915, Medikro Oy, Kuopio, Finland), which had a sampling rate of 100 Hz. Mask (Cortex Personal-Use-Mask, Leipzig, Germany) was attached to the mouthpiece of the spirometer. The spirometer could record at most 1 min long signals.

2.2 Measurement Protocol

The measurements for each patient were done in two parts: 1) short measurement session (5 min) preoperatively; and 2) longer measurement session (3 h) postoperatively.

The first measurements were done in the operating room just before the operation without any sedative premedication. The rib cage respiratory effort belt was placed on the xyphoid process and the abdominal belt was placed above the umbilicus. The mask of the spirometer was put to the volunteer's face and its airtightness was secured. The signals were recorded until two successful recordings of the 1 min were obtained. The places of respiratory effort belts were marked with drawing ink on the skin, so that it was possible to place the belts to the same places postoperatively. The mask and respiratory effort belts were removed.

As soon as it was possible, measurements were continued postoperatively in the recovery room. The rib cage respiratory effort belt and the abdominal respiratory effort belt were placed to the previously marked places. They recorded the signals during the whole 3 hour measurement period. Every 10 min, the mask of the spirometer was put to the volunteer's face, its airtightness was secured and 1 min measurement with the spirometer was recorded. Participation to the study did not affect the routine management of the patients.

2.3 Calculation of Respiratory Airflow Estimates

In this study, we applied our recently published respiratory effort belt calibration method (Seppänen, 2013). The method was therein tested against various breathing style changes and body position changes, and compared with the state-of-the-art methods. Our method outperformed the other methods showing high robustness to the breathing style changes and body position changes.

Our method is an extension to conventional multiple linear regression method so that 1) it uses number N of consecutive input signal samples and linear filtering for estimation of each output signal sample and 2) it is based on polynomial regression to model different transfer functions between the input and output. The method is based on optimally trained FIR (Finite Impulse Response) filter bank constructed as a MISO (Multiple-Input Single-Output) system between the respiratory effort belt signals and the spirometer signal. Three polynomial transfer functions were tested: linear terms only (M1), linear

terms and cross-product term (M2), and linear terms with second order terms (M3).

Figure 1 and equation 1 show the realization of the filter bank for model M2. Similar realizations can be derived also for models M1 and M3.

$$y[k] = \mathbf{a}_1^T \mathbf{x}_1[k] + \mathbf{a}_2^T \mathbf{x}_2[k] + \mathbf{a}_3^T (\mathbf{x}_1[k] \mathbf{x}_2[k]) + \varepsilon[k], \quad (1)$$

where \mathbf{a}_1^T , \mathbf{a}_2^T and \mathbf{a}_3^T denote the N tap coefficients of filters FIR₁, FIR₂ and FIR₃, respectively: $\mathbf{a}_i^T = [a_i[1], a_i[2], \dots, a_i[N]]$, $i = 1, 2, 3$. Superscript T denotes matrix transpose. Parameter y denotes respiratory airflow from spirometer and ε is zero-mean Gaussian error. Vectors \mathbf{x}_1 and \mathbf{x}_2 include N consecutive signal samples from the rib cage respiratory effort signal and abdominal respiratory effort belt signal, respectively: $\mathbf{x}_j[k] = [x_j[k], x_j[k-1], \dots, x_j[k-N+1]]^T$, $j = 1, 2$ and $k = N, \dots, n$. Variable n is the number of observations used in the calibration.

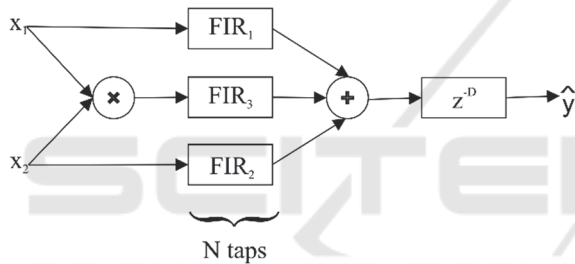


Figure 1: Extended calibration method of respiratory effort belt signals.

\mathbf{X} is an $(n-N+1) \times (3 \times N)$ matrix formed from the vectors \mathbf{x}_1 and \mathbf{x}_2 :

$$\mathbf{X}^T = \begin{bmatrix} \mathbf{x}_1[N] & \dots & \mathbf{x}_1[n] \\ \mathbf{x}_2[N] & \dots & \mathbf{x}_2[n] \\ \mathbf{x}_1[N]\mathbf{x}_2[N] & \dots & \mathbf{x}_1[n]\mathbf{x}_2[n] \end{bmatrix}. \quad (2)$$

During the calibration, tap coefficients \mathbf{a}_1^T , \mathbf{a}_2^T and \mathbf{a}_3^T are estimated with the method of least-squares. The least-squares estimator of the parameter vector $\mathbf{a} = [\mathbf{a}_1^T, \mathbf{a}_2^T, \mathbf{a}_3^T]^T$ is given by

$$\hat{\mathbf{a}} = (\mathbf{X}^T \mathbf{X})^{-1} \mathbf{X}^T \mathbf{y}. \quad (3)$$

The length of the vector $\hat{\mathbf{a}}$ is $3 \times N$. Finally, the respiratory airflow signal estimated from the rib cage and abdominal respiratory effort belt signals through the FIR filter bank is

$$\hat{\mathbf{y}} = \mathbf{X} \hat{\mathbf{a}}. \quad (4)$$

In Figure 1, there is the delay element z^{-D} included at the output. There is always a small delay between the spirometer signal and respiratory effort belt signals

due to the physiological reasons and internal delays of measuring devices. Thus, the signals have to be time-synchronized by searching for a proper value for D (Seppänen, 2013).

We made two different test setups: 1) the data of the second preoperative measurement minute were used to train the estimation model and the data of all the postoperative measurement minutes were used to test the estimation model (PRE setup); and 2) the data of the first postoperative measurement minute were used to train the estimation model and data of the rest postoperative measurement minutes were used to test the estimation model (POST setup).

The similarity of spirometer signals and estimated respiratory airflow signals were assessed by computing R^2 (coefficient of determination) values. Tidal volumes, minute volumes and BPM (Breaths per Minute, respiratory rate) were calculated from the spirometer signals and estimated respiratory airflow signals. Relative errors were calculated.

3 RESULTS AND DISCUSSION

Signals were recorded according to the protocol described in Section 2.2. There were altogether 93 simultaneous measurement minutes with spirometer and respiratory effort belts. Five of these had to be discarded due to a malfunction of the spirometer. One of them had to be discarded due to a malfunction of the polygraphic recorder. In addition to that, five postoperative measurement minutes of patient 5 had to be discarded, because he had serious difficulties to wake up and stay awake in the recovery room. During the measurements patients received opioid analgesia as many times as they needed: 3, 2, 1, 7 and 4 times for patients 1-5, respectively.

During the measurements a number of problems related to PRE setup were observed. Firstly, places of respiratory effort belts can interchange before POST setup by mistake. Secondly, there may be a need to tighten or loosen the respiratory effort belts after the operation, because fluids can accumulate in the body or can leave from the body during the operation. This leads to a situation where the estimation model trained with a preoperative data is not valid anymore. Thirdly, if there are complications during the operation or if the operation is prolonged otherwise, the estimation model trained with a preoperative data can be erroneous for the postoperative data. With the POST setup, no problems were observed.

3.1 Accuracy of Airflow Estimates

The selection of the best model and FIR filter length (N value) depended on whether waveform accuracy (R^2), tidal volume (V_T) error, minute volume (V_{minute}) error or BPM error values were studied. Table 2 summarizes the results when PRE setup was used for training and testing all estimation models. It is seen in Table 2 that model M1 produced the best results.

Table 2: Results (average value \pm SD) with the best models when PRE setup was used for training and testing all estimation models.

Best model	M1	M1	M1	M1
FIR size	N = 8	N = 8	N = 8	N = 16
Patient	R^2	Abs (V_T error) [%]	Abs (V_{minute} error) [%]	BPM error
1	0.88 \pm 0.05	12.8 \pm 10.7	12.5 \pm 9.5	0.03 \pm 0.07
2	0.87 \pm 0.06	26.7 \pm 7.7	25.1 \pm 8.2	0.01 \pm 0.01
3	0.94 \pm 0.02	10.9 \pm 2.9	14.2 \pm 5.0	0.09 \pm 0.30
4	0.87 \pm 0.06	15.9 \pm 6.0	21.7 \pm 8.6	0.09 \pm 1.14
5	0.43 \pm 0.17	70.2 \pm 14.1	72.4 \pm 12.3	0.48 \pm 0.79
Average	0.82 \pm 0.18	24.1 \pm 21.4	26.0 \pm 21.3	0.29 \pm 0.70

Table 3 summarizes the results when POST setup was used for training and testing all estimation models. In this case, it is seen that model M2 produced the best results with this data. As an important difference to the preceding results in Table 2, more accurate waveforms were received since R^2 values were higher and BPM error values lower. Also, the volume error values decreased to the fractions.

Table 3: Results (average value \pm SD) with the best model when POST setup was used for training and testing all estimation models.

Best model	M2	M2	M2	M2
FIR size	N = 8	N = 16	N = 16	N = 8
Patient	R^2	Abs (V_T error) [%]	Abs (V_{minute} error) [%]	BPM error
1	0.90 \pm 0.04	11.4 \pm 7.9	9.9 \pm 6.8	0.01 \pm 0.01
2	0.95 \pm 0.01	5.9 \pm 4.5	5.8 \pm 5.0	0.01 \pm 0.01
3	0.94 \pm 0.04	5.4 \pm 4.7	6.3 \pm 4.2	0.10 \pm 0.30
4	0.88 \pm 0.09	8.7 \pm 6.0	11.9 \pm 10.2	0.83 \pm 1.13
5	0.91 \pm 0.02	10.5 \pm 9.3	8.2 \pm 6.3	0.01 \pm 0.00
Average	0.91 \pm 0.06	5.8 \pm 6.3	8.5 \pm 7.1	0.21 \pm 0.63

It can be seen from Table 2 and Table 3, that if the smallest error results are sought, then there is a need to use several models. However, if there is, for example, a need to get accurate respiratory rate only, then one should choose POST setup and model M2 with N value 8. On the other hand, one may wish to use only one model with good overall performance.

The results for that are presented next. Model M3 (including linear and 2nd order terms) produced clearly worse results than the other models, thus only the results of using models M1 and M2 are presented here. Table 4 and Table 5 present the results when the estimation model M1 with N value 8 was used with PRE and POST setups, respectively.

Table 4: Results (average value \pm SD) of the calibration when estimation model M1 (N = 8) was used with PRE setup.

Patient	R^2	Abs (V_T error) [%]	Abs (V_{minute} error) [%]	BPM error
1	0.88 \pm 0.05	12.8 \pm 10.7	12.5 \pm 9.5	0.09 \pm 0.27
2	0.87 \pm 0.06	26.7 \pm 7.7	25.1 \pm 8.2	0.01 \pm 0.01
3	0.94 \pm 0.02	10.9 \pm 2.9	14.2 \pm 5.0	0.09 \pm 0.29
4	0.87 \pm 0.06	15.9 \pm 6.0	21.7 \pm 8.6	1.00 \pm 1.06
5	0.43 \pm 0.17	70.2 \pm 14.1	72.4 \pm 12.3	0.37 \pm 0.55
Average	0.78 \pm 0.20	24.1 \pm 21.4	26.0 \pm 21.3	0.32 \pm 0.68

Table 6 and Table 7 present the results when the estimation model M2 with N value 8 was used with PRE and POST setups, respectively.

It is clearly seen from Tables 4-7 that POST setup produced superior results. Respiratory airflow waveforms are much more accurate, average R^2 increased from 0.78 to 0.91 with both models M1 and M2. In addition to that, tidal volume errors, minute volume errors and BPM errors are smaller. However, when the average results of Table 5 and Table 7 are compared, it can be seen that models M1 and M2 with N value 8 produced both very good results and that there are little differences between the results.

Table 5: Results (average value \pm SD) of the calibration when estimation model M1 (N = 8) was used with POST setup.

Patient	R^2	Abs (V_T error) [%]	Abs (V_{minute} error) [%]	BPM error
1	0.91 \pm 0.04	11.6 \pm 7.8	8.9 \pm 7.1	0.01 \pm 0.01
2	0.94 \pm 0.02	6.9 \pm 7.0	5.7 \pm 5.6	0.01 \pm 0.01
3	0.94 \pm 0.04	5.6 \pm 4.5	6.0 \pm 3.8	0.10 \pm 0.30
4	0.87 \pm 0.09	8.4 \pm 4.9	11.9 \pm 8.9	0.82 \pm 1.13
5	0.90 \pm 0.02	9.6 \pm 5.3	10.9 \pm 4.9	0.12 \pm 0.35
Average	0.91 \pm 0.06	8.4 \pm 6.1	8.6 \pm 6.7	0.23 \pm 0.64

Table 6: Results (average value \pm SD) of the calibration when estimation model M2 (N = 8) was used with PRE setup.

Patient	R^2	Abs (V_T error) [%]	Abs (V_{minute} error) [%]	BPM error
1	0.82 \pm 0.08	17.8 \pm 9.8	21.3 \pm 8.3	0.10 \pm 0.27
2	0.76 \pm 0.09	42.7 \pm 8.8	51.7 \pm 9.6	0.04 \pm 0.12
3	0.93 \pm 0.03	13.3 \pm 5.1	15.3 \pm 6.4	0.09 \pm 0.30
4	0.87 \pm 0.06	15.4 \pm 6.7	19.6 \pm 8.6	0.91 \pm 1.11
5	0.39 \pm 0.21	55.1 \pm 9.5	65.5 \pm 15.1	1.67 \pm 1.47
Average	0.78 \pm 0.20	26.9 \pm 17.8	32.4 \pm 21.1	0.49 \pm 0.96

3.2 Example Cases

Figure 2 depicts short segment of example signals with low airflow. Estimation model M2 (N = 16) was used with the POST setup for the measurement signals of patient 3. In this case, R² was 0.94, tidal volume error 1.5 %, minute volume error 10.9 % and BPM error 0.01. The spirometer signal is estimated with excellent accuracy.

Figure 3 depicts an example of apneic event. In this case, estimation model M1 (N = 8) was used with the POST setup for the measurement signals of patient 5. During obstruction, the rib cage ceases to move, but abdomen is moving. There is no air exchange, so there is no airflow signal either. It can be seen from the figure, that during the obstruction airflow was zero, but because there was movement in respiratory effort belts, the estimated respiratory airflow signal also showed activity. The same phenomenon was also encountered by Drummond et al., (2013) and Voscopoulos et al., (2013). However, apneic events can be detected from the changed pattern of movements from respiratory effort belt signals. Both of them have lower amplitudes than before or after the apneic event. Especially the rib cage respiratory effort belt is almost motionless during the apneic event. Detected parts of the respiratory airflow estimate could then be replaced with zero airflow.

Table 7: Results (average value ± SD) of the calibration when estimation model M2 (N = 8 was used with POST setup.

Patient	R ²	Abs (V _T error) [%]	Abs (V _{minute} error) [%]	BPM error
1	0.90 ± 0.04	11.4 ± 7.6	10.0 ± 7.0	0.01 ± 0.01
2	0.95 ± 0.01	6.1 ± 4.8	6.2 ± 5.3	0.01 ± 0.01
3	0.94 ± 0.04	5.3 ± 4.5	6.2 ± 4.0	0.10 ± 0.30
4	0.88 ± 0.09	8.8 ± 3.9	11.4 ± 10.1	0.83 ± 1.13
5	0.91 ± 0.02	13.1 ± 8.9	9.6 ± 6.4	0.01 ± 0.00
Average	0.91 ± 0.06	8.8 ± 6.6	8.7 ± 7.1	0.21 ± 0.63

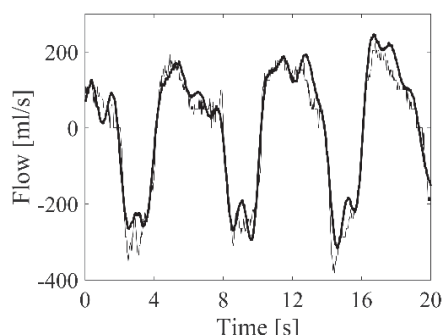


Figure 2: Short segment of example signals with low airflow: spirometer signal (thin line) and the estimated respiratory airflow signal (bold line).

Figure 4 depicts hypopneic event of patient 4 with COPD. Here, estimation model M2 (N = 8) was used with the POST setup. In this case, R² was 0.81, tidal volume error was 0.8 %, minute volume error was 3.24 % and BPM error was 1.08. It can be seen, that the method was able to estimate respiratory airflow very well even in this kind of complicated situations.

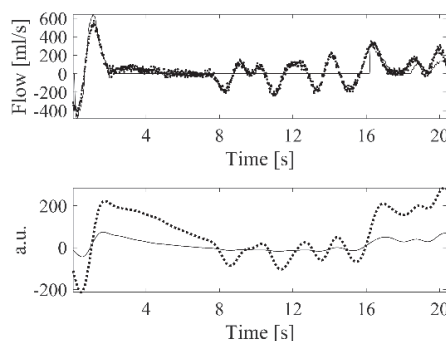


Figure 3: Short segment of example signals during apneic event. Upper subfigure: spirometer signal (solid line) and the estimated respiratory airflow signal (dotted line). Lower subfigure: rib cage respiratory effort belt signal (solid line) and abdominal respiratory effort belt signal (dotted line).

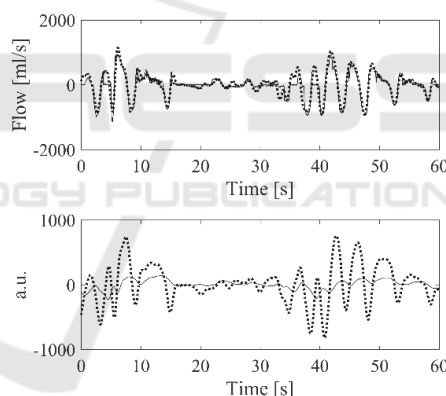


Figure 4: Example signals of COPD patient. Upper subfigure: spirometer signal (solid line) and the estimated respiratory airflow signal (dotted line). Lower subfigure: rib cage respiratory effort belt signal (solid line) and abdominal respiratory effort belt signal (dotted line).

Measurement data of patient 4 included thoracoabdominal asynchrony more or less during the whole measurement session. Figure 5 depicts one example of this. Estimation model M2 (N = 8) was used with the POST setup and the results were the following: R² was 0.94, tidal volume error was 4.7 %, minute volume error was 2.6 % and BPM error was 0.02. These results are consistent with our earlier findings indicating that our method produces very good results with thoracoabdominal asynchrony signals too (Seppänen, 2013).

Figure 6 demonstrates the performance difference between PRE and POST setups. In this case, estimation model M1 ($N = 16$) was used firstly with the PRE setup and secondly with the POST setup. The measurement data was from patient 1. It can be seen from Figure 6 that there were clear differences with the estimated respiratory airflows (PRE setup with dotted line and POST setup with bold line). Following numerical results demonstrate these differences further. The results for the PRE setup were: R^2 was 0.82, tidal volume error was 34.8 %, minute volume error was 35.8 % and BPM error was 0.00. Equivalently results for the POST setup were: R^2 was 0.93, tidal volume error was 14.6 %, minute volume error was 13.9 % and BPM error was 0.00. Although, the PRE setup was otherwise remarkably worse than POST setup in this case, BPM was estimated very accurately.

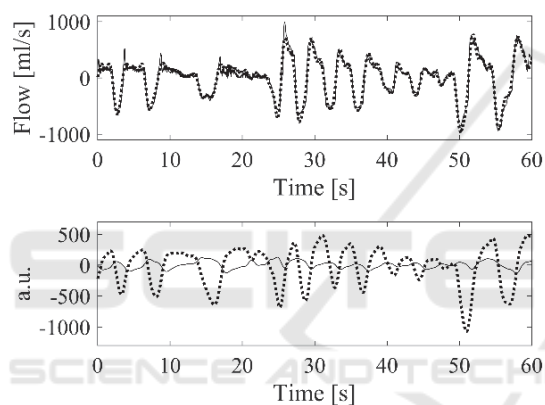


Figure 5: Example signals of thoracoabdominal asynchrony. Upper subfigure: spirometer signal (solid line) and the estimated respiratory airflow signal (dotted line). Lower subfigure: rib cage respiratory effort belt signal (solid line) and abdominal respiratory effort belt signal (dotted line).

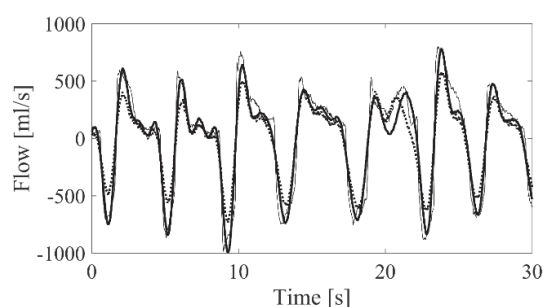


Figure 6: Short segment of example signals depicting the difference of PRE and POST setups: spirometer signal (thin line), the first estimated respiratory airflow signal (PRE setup, dotted line) and the second estimated respiratory airflow (POST setup, bold line).

3.3 Limitations of Study

The study included a number of limitations. Firstly, the study included only five patients. The study should be repeated with a larger data set in order to draw more general conclusions. Secondly, respiratory effort belts cannot be used if the surgical wound is in the area where the belts are placed. However, the proposed method could be applied to the measurement data acquired with other sensors without this kind of restriction, such as acceleration sensors. Thirdly, as was pointed out in *Section 3.2* during the apneic event there is no respiratory airflow but still estimated respiratory airflow shows otherwise. This could be resolved by detecting the changed pattern of movements from respiratory effort belts and replacing these parts of the respiratory airflow estimate with zero airflow. This remains future work.

4 CONCLUSIONS

Here, a method was proposed to estimate accurate continuous respiratory airflow postoperatively. The data from respiratory effort belts were calibrated with a spirometer using an extended multiple linear regression method. The results showed that training the estimation model with the postoperative data produced much more accurate results than training the estimation model with the preoperative data.

It was demonstrated with data from five different patients in postoperative situation that estimated respiratory airflow signals have very accurate waveforms. In addition, tidal volume, minute volume and respiratory rate can be calculated remarkably accurately from these signals. The method produced very good estimates even from challenging respiration signals: low airflows, COPD, hypopneic events and thoracoabdominal asynchrony.

In summary, the presented method is able to produce estimates of postoperative respiratory airflow waveforms to enable accurate, continuous, non-invasive respiratory monitoring postoperatively.

ACKNOWLEDGEMENTS

Finnish Cultural Foundation, North Ostrobothnia Regional Fund and International Doctoral Programme in Biomedical Engineering and Medical Physics (iBioMEP) are gratefully acknowledged for financial support.

REFERENCES

- Cepeda M.S., Farrar J.T., Baumgarten M., Boston R., Carr D.B., Strom B.L., 2003. Side effects of opioids during short-term administration: Effect of age, gender, and race. *Clinical Pharmacology & Therapeutics*, 74(2): 102-112.
- Drummond G.B., Bates A., Mann J., Arvind D.K., 2013. Characterization of breathing patterns during patient-controlled opioid analgesia. *British Journal of Anaesthesia*, 111(6): 971-978.
- Etches R., 1994. Respiratory depression associated with patient-controlled analgesia: a review of eight cases. *Canadian Journal of Anaesthesia*, 41(2): 125-132.
- Gamil M., Fanning A., 1991. The first 24 hours after surgery. A study of complications after 2153 consecutive operations. *Anaesthesia*, 46: 712-715.
- George J.A., Lin E.E., Hanna M.N., Murphy J.D., Kumar K., Ko P.S., Wu C.L., 2010. The effect of intravenous opioid patient-controlled analgesia with and without background infusion on respiratory depression: a meta-analysis. *Journal of Opioid Management*, 6(1): 47-54.
- Lovett P.B., Buchwald J.M., Sturmann K., Bijur P., 2005. The vexatious vital: neither clinical measurements by nurses nor an electronic monitor provides accurate measurements of respiratory rate in triage. *Annals of Emergency Medicine*, 45(1): 68-76.
- Lynn L.A., Curry J.P., 2011. Patterns of unexpected in-hospital deaths: a root cause analysis. *Patient Safety in Surgery*, 5:3.
- Ramsay M.A.E., Usman M., Lagow E., Mendoza M., Untalan E., De Vol E., 2013. The accuracy, precision and reliability of measuring ventilatory rate and detecting ventilatory pause by rainbow acoustic monitoring and capnometry. *Anesthesia & Analgesia*, 117(1): 69-75.
- Seppänen, T.M., Alho, O.-P., Seppänen T., 2013. Reducing the airflow waveform distortions from breathing style and body position with improved calibration of respiratory effort belts. *Biomedical Engineering Online*, 12:97.
- Taylor S., Kirton O.C., Staff I, Kozol R.A., 2005. Postoperative day one: a high risk period for respiratory events. *The American Journal of Surgery*, 190(5): 752-756.
- Voscopoulos C.J., MacNabb C.M., Brayanov J., Qin L., Freeman J., Mullen G.J., Ladd D., George E., 2015. The evaluation of a non-invasive respiratory volume monitor in surgical patients undergoing elective surgery with general anesthesia. *Journal of Clinical Monitoring and Computing*, 29(2): 223-230.
- Voscopoulos C., Ladd D., Campana L., George E., 2014. Non-invasive respiratory volume monitoring to detect apnea in post-operative patients: case series. *Journal of Clinical Medicine Research*, 6(3): 209-214.
- Voscopoulos C.J., MacNabb C.M., Freeman J., Galvagno S.M., Ladd D., George E., 2014. Continuous noninvasive respiratory volume monitoring for the identification of patients at risk for opioid-induced respiratory depression and obstructive breathing patterns. *Journal of Trauma and Acute Care Surgery*, 77(3): S208-S215.
- Voscopoulos C, Brayanov J., Ladd D., Lalli M., Panasyuk A., Freeman J., 2013. Evaluation of a novel noninvasive respiration monitor providing continuous measurement of minute ventilation in ambulatory subjects in a variety of clinical scenarios. *Anesthesia & Analgesia*, 117(1): 91-100.